Chemical Engineering Journal 228 (2013) 1148–1157

Contents lists available at SciVerse ScienceDirect

Chemical Engineering Journal

journal homepage: www.elsevier.com/locate/cej

Nitrobenzene degradation in Fenton-like systems using Cu(II) as catalyst. Comparison between Cu(II)- and Fe(III)-based systems

Daniela A. Nichela [a,b], Andrea M. Berkovic [a,c,*], Mariana R. Costante [a], María P. Juliarena [c], Fernando S. García Einschlag [a,*]

[a] Instituto de Investigaciones Fisicoquímicas Teóricas y Aplicadas (INIFTA), Facultad de Ciencias Exactas, Universidad Nacional de La Plata, C.C. 16, Suc. 4, 1900 La Plata, Argentina
[b] Instituto Investigaciones Biodiversidad y Medio Ambiente (INIBIOMA, CONICET), Centro Regional Universitario Bariloche, Universidad Nacional del Comahue, Quintral 1250, 8400 Bariloche, Argentina
[c] Instituto de Física "Arroyo Seco" (IFAS), IFAS-UNICEN, Pinto 399, 7000 Tandil, Argentina

HIGHLIGHTS

- Cu^{2+} can be as effective as Fe^{3+} for catalyzing NBE oxidation in Fenton-like systems.
- TOC reductions were higher in the presence of Cu^{2+}.
- Cu^{2+} is catalytically active in a wide range of pH values around neutrality.
- Cu^{2+} exhibits high apparent activation energy above 35 °C.
- The highly toxic product 1,3-dinitrobenzene was not detected in Cu^{2+}-based systems.

ARTICLE INFO

Article history:
Received 14 December 2012
Received in revised form 8 April 2013
Accepted 4 May 2013
Available online 15 May 2013

Keywords:
Nitrobenzene
Copper(II)
Iron(III)
Fenton-like
Photo-enhancement

ABSTRACT

Nitrobenzene (NBE) degradation in Fenton-like systems using copper(II) as catalyst was investigated and compared with the trends observed in iron(III)-based systems. UV–vis spectroscopy, HPLC and TOC measurements were used to characterize the evolution of the reaction mixtures. Kinetic profiles were analyzed under a wide range of experimental conditions in order to assess the effects of the reaction temperature, initial concentrations and working pH. For both Cu(II)-based and Fe(III)-based systems, treatment times decreased with increasing oxidant and catalyst concentrations, but augmented with increasing NBE concentration. However, significant differences were observed for Cu(II)-based systems: higher activation energy above room temperature, broader pH range of activity with an optimal pH of about 6.2, absence of 1,3-dinitrobenzene among the reaction products and important reductions in the TOC levels even in the absence of irradiation.

1. Introduction

Advanced oxidation technologies (AOTs) are based on the production of strongly oxidizing species such as hydroxyl radicals ($HO^{\cdot}$) and have been broadly applied for the elimination of recalcitrant pollutants during the past two decades [1–4]. Among the AOTs, Fenton reagent combines ferrous salts (Fe(II)) with hydrogen peroxide (H_2O_2), whereas Fenton-like processes involve a series of thermal reactions catalyzed by transition metal salts (frequently ferric salts, hereafter represented as Fe(III)), that lead to H_2O_2 decomposition. The classical mechanism for Fenton processes identifies the hydroxyl radical ($HO^{\cdot}$) as the main reactive species [4–6]. The set of chain reactions involved in the production and decay of $HO^{\cdot}$ in Fenton and Fenton-like systems has been the subject of many studies [1,5–9]. The classic Fenton reagent yields $HO^{\cdot}$ radicals through the following process:

$$Fe(II) + H_2O_2 \rightarrow Fe(III) + HO^{\cdot} + HO^{-} \quad (R1a)$$

It has been reported that Cu(I) in aqueous solution may behave as a "Fenton-like" catalyst [10–12] since hydroxyl radicals can be generated by the reaction

$$Cu(I) + H_2O_2 \rightarrow Cu(II) + HO^{\cdot} + HO^{-} \quad (R1b)$$

The highly reactive hydroxyl radicals generated may react with the target substrates (S) or with the oxidant itself

* Corresponding authors. Address: Instituto de Investigaciones Fisicoquímicas Teóricas y Aplicadas (INIFTA), Facultad de Ciencias Exactas, Universidad Nacional de La Plata, C.C. 16, Suc. 4, 1900 La Plata, Argentina. Tel.: +54 249 4439660/1; fax: +54 249 439669 (A.M. Berkovic), tel.: +54 221 4257430; fax: +54 221 4254642 (F.S. García Einschlag).
E-mail addresses: a_berkovic@yahoo.com (A.M. Berkovic), fgarciae@quimica.unlp.edu.ar (F.S. García Einschlag).

1385-8947/$ - see front matter © 2013 Elsevier B.V. All rights reserved.
http://dx.doi.org/10.1016/j.cej.2013.05.002

$$HO^{\cdot} + S \rightarrow \text{Products} \quad (R2)$$

$$HO^{\cdot} + H_2O_2 \rightarrow HO_2^{\cdot} + H_2O \quad (R3)$$

Previous AOT studies [1,13–15] have confirmed that an essential design parameter is the fraction of $HO^{\cdot}$ scavenged by hydrogen peroxide. Hence, high H_2O_2 concentrations should be avoided to keep the contribution of reaction 3 as small as possible.

In order to complete the catalytic cycle, the oxidized forms of the metal cations should be reduced. In the absence of other reducing species, the main pathway for Fe(II) regeneration in nonirradiated systems is the overall reaction [5,15]

$$Fe(III) + H_2O_2 \rightarrow Fe(II) + HO_2^{\cdot} + H^+ \quad (R4a)$$

A similar reduction mechanism has been reported for Cu(II) [16–19]

$$Cu(II) + H_2O_2 \rightarrow Cu(I) + HO_2^{\cdot} + H^+ \quad (R4b)$$

Given that the rate constants associated with reactions (1a) and (1b) are much larger than those associated with reactions (4a) and (4b) [1,4,15,18,20], the catalytic cycles are usually limited by the reduction of the Fe(III) and Cu(II), respectively.

Besides hydrogen peroxide, the hydroperoxide radical ($HO_2^{\cdot}$) and superoxide radical anion ($O_2^{\cdot-}$) are among the most important inorganic species capable of reducing the oxidized forms of the metal cations in aqueous media [1,4,9,18–20]

$$Fe(III) + HO_2^{\cdot} \rightarrow Fe(II) + H^+ + O_2 \quad (R5a)$$

$$Cu(II) + HO_2^{\cdot} \rightarrow Cu(I) + H^+ + O_2 \quad (R5b)$$

$$Fe(III) + O_2^{\cdot-} \rightarrow Fe(II) + O_2 \quad (R6a)$$

$$Cu(II) + O_2^{\cdot-} \rightarrow Cu(I) + O_2 \quad (R6b)$$

Superoxide may be formed either by deprotonation of hydroperoxide ($HO_2^{\cdot} \leftrightarrow O_2^{\cdot-} + H^+$) or by electron-transfer reactions between the reduced forms of the metal catalysts and dissolved oxygen ($Fe(II) + O_2 \rightarrow Fe(III) + O_2^{\cdot-}$; $Cu(I) + O_2 \rightarrow Cu(II) + O_2^{\cdot-}$) [21]. Under typical conditions of Fenton-like systems, the contribution of the latter reactions is expected to be of minor importance since Fe(II) and Cu(I) are rapidly oxidized in the presence of relatively high H_2O_2 concentrations (Reactions 1a and 1b). For both systems, the rate constants associated with the superoxide radical anion are larger than those associated to the hydroperoxyl radical [4,9,20,22].

It is important to note that, during Fenton-like treatments, some reducing organic intermediates (HR) may also be formed [15,23,24]

$$Fe(III) + HR \rightarrow Fe(II) + H^+ + R^{\cdot} \quad (R7a)$$

$$Cu(II) + HR \rightarrow Cu(I) + H^+ + R^{\cdot} \quad (R7b)$$

These mechanisms have been proposed for a variety of aqueous biochemical and chemical systems, seawater and other natural waters. Iron and copper are abundant elements in the environment and coexist in natural waters [21]. Both have a similar photoredox behavior, highly dependent on environmental conditions. Therefore Cu(II) has been tested as an alternative to Fe(III) for catalyzing Fenton-like processes [11,25–28]. Several Cu(II)-catalyzed systems have been a subject of research including benzene, toluene, ethylbenzene, and xylenes (BTEX) degradation using copper complexes and H_2O_2 [27], the reduction of Cu(II) by hydrogen peroxide in natural environments [9], dye decolorization in homogeneous copper(II)/organic acid/hydrogen peroxide systems [28], the photolysis of copper complexes in the presence of oxygen in seawater [21], solar detoxification of metal finishing effluents [29], photo-Fenton elimination of pesticides [12] and the use of copper-based heterogeneous catalysts [11], among others.

In a previous paper [15] we reported the oxidation kinetics of nitrobenzene (NBE) in Fe(III)-based Fenton-like systems. Nitrobenzene (NBE) is one of the most representative nitroaromatic compounds because of its extensive use, high toxicity and chemical stability [30–33]. It is used in large amounts for the industrial production of aniline, lubricating oils, dyes, medicines, pesticides and synthetic rubber [34]. The U.S. *Environmental Protection Agency* (EPA) recommends that NBE levels in lakes and water streams should be limited to 17 ppm to avoid potential health effects as a result of drinking water or eating contaminated fish. In this work, we analyze the ability of Cu(II) for catalyzing the H_2O_2-mediated oxidation of NBE over a wide range of experimental conditions. Furthermore, the effects of operating conditions, i.e., reaction temperature, initial concentrations, working pH and photostimulation, on the main kinetic and mechanistic trends, observed in the presence of each catalyst, are comparatively analyzed.

2. Materials and methods

2.1. Materials

Nitrobenzene (99.5%, Fluka), 1,3-dinitrobenzene (99%, Merck), 2-nitrophenol (99%, Riedel de Haën), 3-nitrophenol (99%, Riedel de Haën), 4-nitrophenol (99%, Riedel de Haën), H_2O_2 (Perhydrol, 30% Merck), H_2SO_4 (98%, Merck), K_2HPO_4 (99%, Merck), KH_2PO_4 (99%, Merck), $Fe(ClO_4)_3{\cdot}H_2O$ (chloride < 0.01%, Aldrich), NaOH (99%, Merck) and $CuSO_4{\cdot}5H_2O$ (99%, Merck), H_3PO_4 (85%, Aldrich), $HClO_4$ (71%, Merck), and triethylamine (TEA, J.T. Baker 100%) were used without further purification. Acetonitrile HPLC grade was purchased from Merck. Nitrogen, oxygen and analytic air were supplied by AGA. Deionized water (>18 MΩ cm and <20 ppb of organic carbon) was obtained from a Millipore system.

2.2. Analytical techniques

Quantification of the substrate and the primary degradation intermediates in the reaction mixtures was performed by HPLC using a Shimadzu instrument (solvent delivery module LC-20AT, online degasser DGU-20A5, UV–vis photodiode array detector SPD-M20A, column oven CTO-10 A5 VP, autosampler SIL-20AAT) equipped with an Alltech Prevail Organic Acid column (RP-C18, 150 mm long × 4.6 mm i.d.). The column temperature was maintained at 25 °C. The mobile phases were prepared by mixing different proportions of ACN with an aqueous buffer at pH 3.0 (11 mM H_3PO_4 and 6.4 mM triethylamine). Two mobile phases, composed of 35/65 and 30/70 (v/v) ACN/aqueous buffer, were used. The first mobile phase, with a shorter NBE retention time, was used to follow the NBE concentration profile in kinetic studies. The second mobile phase, which yielded longer chromatographic runs but with higher peak resolution for 2-nitrophenol, 3-nitrophenol, 4-nitrophenol and 1,3-dinitrobenzene, was used to analyze the product distributions. The flow rate was 1 mL/min and the detection wavelength was set to 265 nm.

Absorption spectra were recorded with either a Varian spectrophotometer (Cary 3) or a Shimadzu spectrophotometer (UV-1800), and using quartz cells of 0.2 or 1.0 cm optical path. The pH of the solutions was monitored using a Radiometer pH-meter (model PHM220).

The H_2O_2 concentration was measured by an enzymatic-colorimetric method employing a commercial kit from Wiener for cholesterol quantization [35]. Aliquots of 50 μl of the reaction mixture were added to 2 mL of reagent and left for 30 min at room

temperature (i.e., 24 ± 3 °C); subsequently the absorption spectra were recorded from 400 to 600 nm. The corresponding calibration curves were constructed using commercial H_2O_2 standards.

2.3. Experimental procedures

All experiments were conducted in a 500-mL glass reactor (Scheme S1, Supplementary material), at controlled temperature (Thermostat MGW Lauda ±0.2 °C) and with constant stirring. Photochemical experiments were performed in the same reactor under continuous supply of analytic air and using a medium pressure mercury lamp (Philips 125 W HPK) installed within a Pyrex sleeve with a cut-off wavelength of 310 nm. The emission spectrum of the lamp was reported elsewhere [36]. The incident photon rate, measured using potassium ferrioxalate as actinometer [37] at 25 °C was 1.39×10^{-6} Eins s^{-1} L^{-1}.

The pH of solutions was adjusted to a value of 3.0 for Fe(III)-based systems and between 3.0 and 7.0 for Cu(II)-based systems using 0.1 M solutions of $HClO_4$ or NaOH. The concentrations of Cu(II), Fe(III), NBE, and H_2O_2 varied from 0.01 to 5.1 mM, 0.014 to 1.0 mM, 0.24 to 2.4 mM, and 1.2–53 mM, respectively. The evolution of the total organic carbon (TOC) was monitored using a Shimadzu instrument (5000A TOC analyzer, catalytic oxidation on Pt at 680 °C). Cu(II) and Fe(III) containing solutions were brought to pH = 8.0 and then filtered before TOC analysis. Prior to injection, all samples were filtered through 0.45 μm nylon filters. Experimental results showed good reproducibility. Runs were repeated 2 or 3 times under identical conditions. The standard relative deviations obtained were, in all cases, smaller than 13.6%.

3. Results and discussion

3.1. Comparison of kinetic profiles obtained in the presence of each catalyst

The kinetic profiles of NBE oxidation in the presence of H_2O_2 and catalytic amounts of either Cu(II) or Fe(III) were analyzed for a wide range of experimental conditions. In order to study the kinetics of NBE transformation we used the absorbance profiles recorded at 265 nm (i.e., where NBE displays an absorption maximum) since they are closely correlated with the NBE concentration profiles obtained by HPLC [15]. Fig. 1 shows the kinetic profiles, expressed as normalized values (i.e., $Abs\text{-}265_{Norm} = Abs_{265}(t)/Abs_{265}(0)$), obtained using both catalysts under the reaction conditions typically used for iron-based Fenton-like systems.

The results demonstrate that, under the conditions tested, copper(II)-based systems show negligible activity. Taking into account previous reports indicating that copper-based systems show higher activity at pH values above 4.5 [18,29,38,39], an additional experiment of NBE degradation was performed using the same conditions but setting the initial pH at a value of 5.0. As expected, an increase in the reaction rate was observed when the copper(II)-catalyzed system was operated at pH 5.0. However, it is clear that under the working conditions tested, the copper(II)-based system cannot be considered as an alternative to the iron(III)-based system from a technical viewpoint.

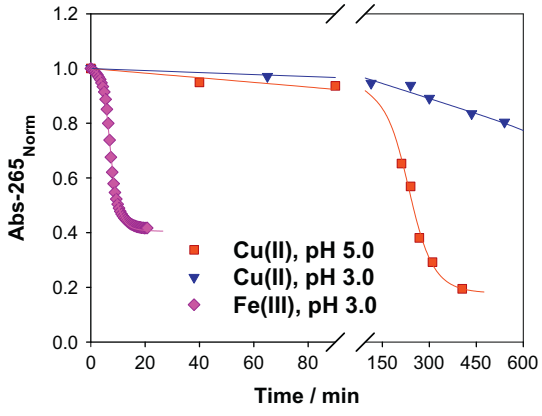

Fig. 1. Kinetic profiles of NBE transformation in Fenton-like systems based on iron or copper as catalysts: [catalyst] = 1.0 mM, [NBE] = 1.2 mM, [H_2O_2] = 50 mM and 30 °C.

Inspection of NBE degradation profiles indicates that both systems display autocatalysis since the degradation rates (associated with the slope of the kinetic traces) increase with time up to conversion degrees as high as 60%. In order to further clarify the autocatalytic nature of the studied systems, we analyzed the instantaneous NBE degradation rates (estimated as $\Delta Abs/\Delta t$ for each time interval) for two additional experiments, which are representative of the kinetic profiles obtained in the presence of each catalyst (Fig. S1, Supplementary material). Although autocatalysis is usually less evident in the presence of copper than in the presence of iron, in both systems, the plots of the reaction rates against time yielded profiles that are typical of autocatalytic processes [40]. This behavior has been attributed to the accumulation of organic reducing intermediates, formed as the reaction proceeds, that participate in reactions such as (R7a) and (R7b) [15,23,41,42].

For both systems, a final phase is observed where the spectral changes are much less evident. HPLC measurements showed that this phase is reached for NBE conversion degrees higher than 90%. Noteworthy, the residual absorbance values during the final phase are much higher for the iron-catalyzed system than for the copper-catalyzed system. This suggests a higher degree of mineralization in the copper-based system and will be discussed below (Section 3.5).

It is well known that, for iron(III)-based Fenton-like treatments, the degradation efficiency may be strongly dependent on the operating conditions [15]. Since the aim of this work was to analyze the potential application of Cu(II)-based systems, we performed a detailed characterization of Cu(II)-based systems using reaction conditions that allow achieving reasonable timescales for NBE treatment. The strategies used to accelerate NBE treatment in the presence of copper(II) include the use of higher oxidant and catalyst concentrations, the use of pH values above 4.5, the increase of the working temperature and the photostimulation of the process. The trends obtained in copper(II)-based systems are compared from a technological viewpoint with those typically found in iron(III)-based systems.

3.2. Effect of temperature on the kinetics of NBE degradation

In order to analyze the effect of working temperature on NBE degradation efficiency in copper(II)-catalyzed systems, a set of experiments was conducted using 50 mM of H_2O_2, 1.2 mM of NBE, 5 mM of Cu(II), and pH 5.0. Fig. 2 shows the normalized kinetic profiles obtained at different temperatures and the corresponding Arrhenius plot.

As expected, a temperature increase decreases the treatment time (Fig. 2a). The Arrhenius plots for the initial rates of NBE transformation reveal that the apparent activation energy (AE) changes at around 35 °C (Fig. 2b). This behavior suggests a complex reaction mechanism that involves several stages whose relative contributions depend on the temperature range analyzed. Below 35 °C, an apparent activation energy of about 12.6 (±0.5) kcal/mol is obtained from the slope, whereas above 35 °C the calculated value is 27.3 (±0.8) kcal/mol. This latter value is rather close to the activation energy reported by Millero et al. for reaction 4b (i.e., 29.9 kcal/mol) [18] and supports the hypothesis that (R4b) is one of the rate limiting steps for copper(II)-catalyzed systems.

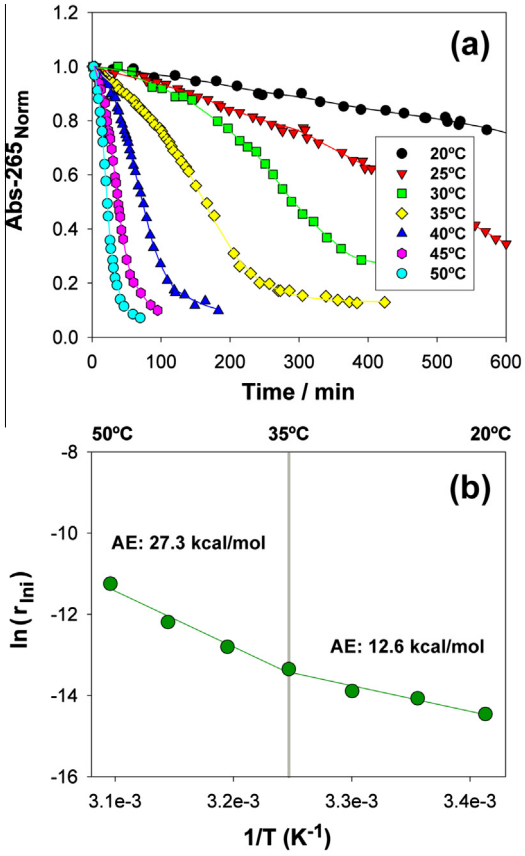

Fig. 2. (a) Profiles of NBE degradation at different temperatures. [Cu(II)] = 5.0 mM, [H_2O_2] = 50 mM, [NBE] = 1.2 mM, and pH = 5.0. (b) Arrhenius plot for the initial NBE degradation rates and estimations of the apparent activation energies.

At this point it is important to recall that we have previously reported a value of 7.5 (±0.4) kcal/mol for the experimental activation energy of NBE degradation above 25 °C in Fe(III)-based Fenton-like systems [15]. The much higher apparent activation energy in the presence of Cu(II) indicates that an increase in the operation temperature above 35 °C would have a much higher efficiency enhancement in copper(II)-based systems than in iron(III)-based systems. This has important consequences from a practical viewpoint and will be considered in Section 3.6.

3.3. Effect of the initial concentrations on the kinetic profiles of NBE degradation

The effects of the initial concentrations on NBE decay were evaluated at about room temperatures. In order to achieve timescales of comparable order Cu(II)-based systems were tested at pH 5.0 and 30 °C, whereas Fe(III)-based systems were studied at pH 3.0 and 20 °C. Despite the significant differences in the reaction conditions and in the NBE treatment times, the general trends observed for the Cu(II)-catalyzed systems (Fig. 3a–c) were similar to those obtained for the Fe(III)-catalyzed systems (Fig. 3d and f).

Given the complexity of the profiles observed and in order to quantitatively compare the kinetic trends between both systems, we used an empirical equation [24] capable of describing the decay profiles with inverted S-shape usually found in Fenton-like systems. The solid curves drawn along with the kinetic profiles (Figs. 1–6) were obtained by fitting the experimental data to Eq. (8).

$$f = \frac{(1 - a \times t - d)}{1 + (t/b)^c} + d \tag{8}$$

Table 1
Effect of initial concentrations on NBE half-life. Cu-catalyzed systems were tested at pH 5.0 and t = 30 °C; whereas Fe-catalyzed systems were tested at pH 3.0 and t = 20 °C.

Variable	[Cu(II)]/(M)	[H_2O_2]/(M)	[NBE]/(M)	$t^{½}$ (min)	ξ
[Cu(II)]	5×10^{-3}	0.052	1.22×10^{-3}	154	0.35
	1×10^{-3}	0.052	1.22×10^{-3}	270	
[NBE]	5×10^{-3}	0.052	2.44×10^{-3}	457	−1.57
	5×10^{-3}	0.052	1.22×10^{-3}	154	
[H_2O_2]	5×10^{-3}	0.052	1.22×10^{-3}	154	1.39
	5×10^{-3}	0.010	1.22×10^{-3}	1525	
	[Fe(III)]/(M)	[H_2O_2]/(M)	[NBE]/(M)	$t^{½}$ (min)	ξ
[Fe(III)]	4.1×10^{-4}	7.75×10^{-3}	1.22×10^{-3}	49	0.60
	7.6×10^{-5}	7.75×10^{-3}	1.22×10^{-3}	134	
[NBE]	3.0×10^{-4}	7.75×10^{-3}	1.22×10^{-3}	17	−2.16
	3.0×10^{-4}	7.75×10^{-3}	2.44×10^{-3}	76	
[H_2O_2]	1.5×10^{-4}	1.24×10^{-2}	2.43×10^{-4}	39	0.43
	1.5×10^{-4}	1.24×10^{-3}	2.43×10^{-4}	106	

In this equation, the parameters a, b, *c* and *d* can be used to represent the main features of the kinetic profiles: the average initial decay rate, the apparent half-life, the average slope during the fast phase and the final residual value, respectively. Table S1 in the Supplementary material lists the values of the parameters that describe the kinetic profiles shown in Fig. 3.

Since the concentration profiles do not follow a simple kinetic behavior, we used NBE half-life ($t^{½}$) in order to roughly characterize the overall treatment rates by a single parameter. Table 1 shows the values of $t^{½}$ obtained in the presence of each catalyst using different initial concentrations. With the purpose of semi-quantitatively evaluating the effects of the initial concentrations on the overall treatment rates, Table 1 also lists the sensibility factors (ξ), which were calculated as:

$$\xi = \frac{\ln\left(t_1^{1/2}/t_2^{1/2}\right)}{\ln(c_2/c_1)} \tag{9}$$

where $t_1^{\frac{1}{2}}/t_2^{\frac{1}{2}}$ represents the ratio of NBE half-lives and c_2/c_1 is the ratio of the initial concentration that was changed between two runs. Hence, the values listed in the last column of Table 1 illustrate the variation of the process timescale between two kinetic runs performed keeping all but one of the concentrations constant and roughly account for the effect of varying the initial concentration of a particular component of the reaction mixture on the overall treatment rate.

The values presented in Table 1 quantify the trends observed in Fig. 3. Independently of the catalyst considered, the increase in catalyst or H_2O_2 concentrations leads to a decrease in the half-lives, whereas a higher substrate concentration leads to an increase in the treatment time. However, there are important differences in the sensibility of each system because the effects of catalyst and substrate concentration are more pronounced for Fe(III)-based systems than for Cu(II)-based systems, whereas the relative effect of oxidant concentration is more pronounced for Cu(II)-based systems than for Fe(III)-based systems. It is important to note that, given the toxicity of Cu(II), the relatively low sensibility of copper(II)-catalyzed systems to a decrease in Cu(II) concentration has important consequences for potential applications.

3.4. HPLC analysis of reaction intermediates

A detailed study of the distribution of primary NBE transformation products in the presence of iron salts for both Fenton and Fenton-like systems was recently reported [43]. Among the primary reaction products, 4-nitrophenol (4NP), 3-nitrophenol

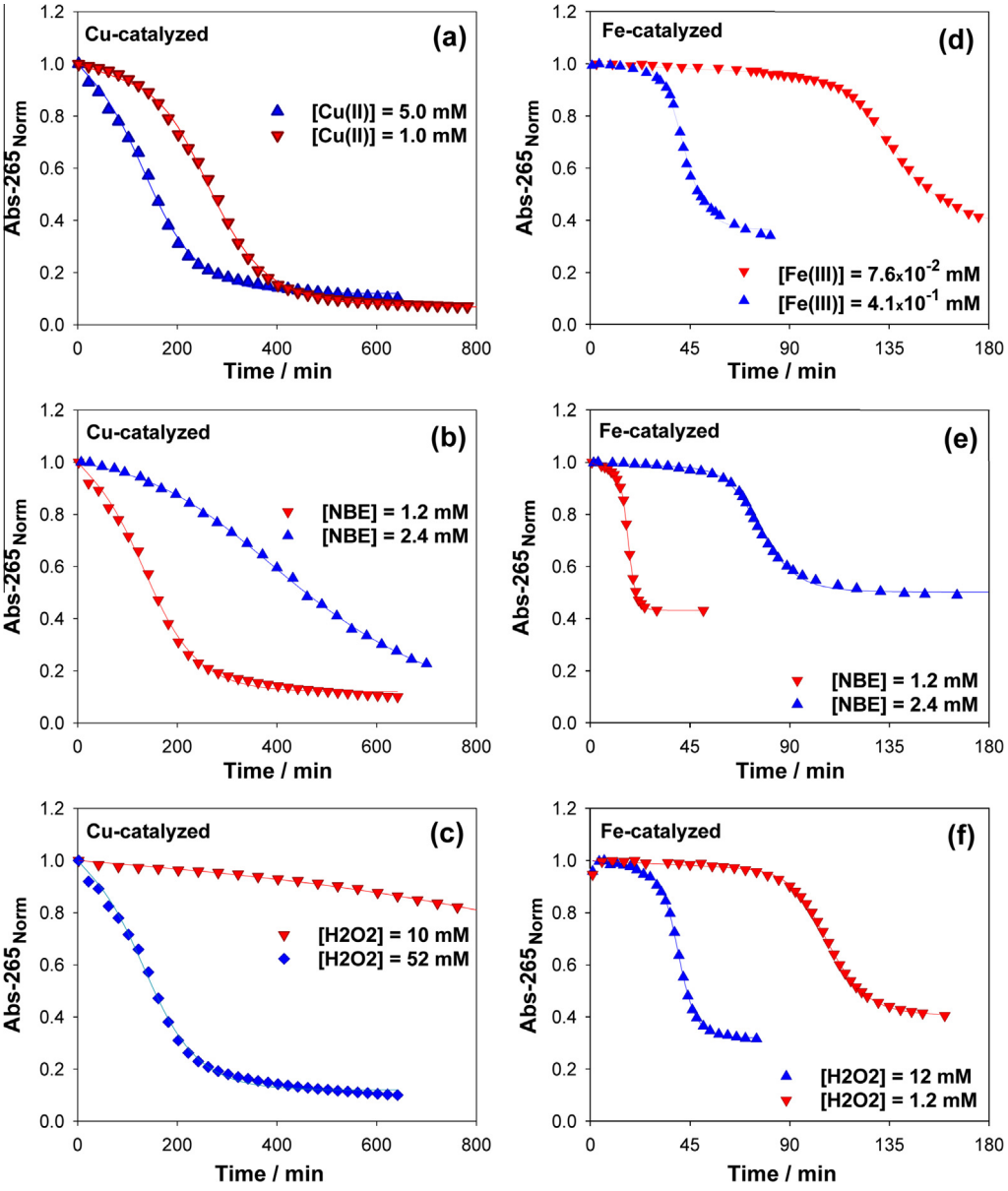

Fig. 3. Effects of varying initial concentrations on the kinetic profiles. Cu(II)-catalyzed systems were tested at pH 5.0 and t = 30 °C; whereas Fe(III)-catalyzed systems were tested at pH 3.0 and t = 20 °C. (a) [NBE] = 1,2 mM and [H_2O_2] = 50 mM; (b) [Cu(II)] = 5 mM and [H_2O_2] = 50 mM; (c) [Cu(II)] = 5 mM and [NBE] = 1.2 mM; (d) [NBE] = 1,2 mM and [H_2O_2] = 7.8 mM; (e) [Fe(III)] = 0.3 mM and [H_2O_2] = 7.8 mM; (f) [Fe(III)] = 0.15 mM and [NBE] = 0.24 mM.

(3NP), 2-nitrophenol (2NP), 1,3-dinitrobenzene (DNB) and also trace amounts of phenol, were detected. It was found that the relative yields were significantly dependent on Fe^{+2}, Fe^{+3}, H_2O_2 and O_2 concentrations [43]. Given that DNB is about 30–50 times more toxic than NBE, the mechanism and the conditions that favor the formation of DNB were further studied [44]. In the present work, HPLC analyses were performed in order to compare the product distributions obtained for Cu(II) and Fe(III)-catalyzed systems. Table 2 lists the relative yields of the three nitrophenol isomers (η^N) as well as the maximum (peak) DNB concentration obtained during NBE degradation runs performed under different working conditions.

The experiments shown in Table 2 are grouped in three subsets: entries 1–3 compare the product distribution obtained in the presence of each catalyst at 30 °C using identical initial concentrations and also evaluate the effect of a pH change for the copper(II)-catalyzed system; entries 4–7 assess the effect of dissolved oxygen on product distribution under conditions that allow obtaining comparable timescales for both catalysts at about room temperature; and entries 8–11 evaluate the effect of irradiation on both systems operated at 60 °C using identical initial concentrations.

The results show that DNB is formed in iron(III)-catalyzed systems for all the conditions tested. In line with previously reported results [44], the production of DNB increases with NBE degradation rate and with iron(III) concentration, but decreases in the presence of dissolved oxygen. In contrast to what is observed for Fe(III)-based Fenton-like systems, in the presence of Cu(II) no detectable amounts of 1,3-DNB were produced under the entire experimental range tested. Given the relatively high toxicity of 1,3-DNB, these results are of major relevance from an environmental viewpoint.

Inspection of the values listed in Table 2 shows that relative nitrophenol yields are in general less sensitive to the reaction con-

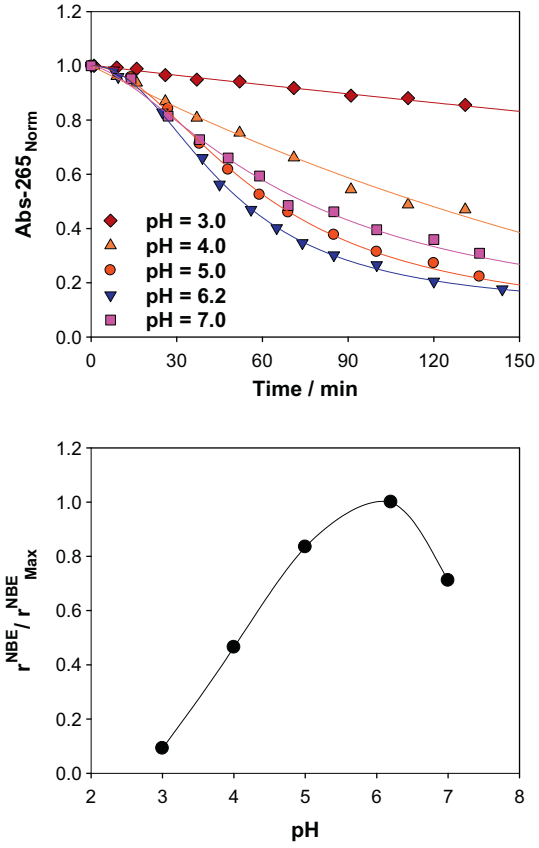

Fig. 4. (a) Kinetic profiles of NBE degradation obtained at different initial pH values using Cu(II) as catalyst. Initial reaction conditions: [NBE] = 1.2 mM, [H_2O_2] = 50 mM, [Cu(II)] = 0.01 mM and t = 60 °C. (b) Normalized overall NBE degradation rate against initial pH (r^{NBE} values were estimated as $1/t^{½}$).

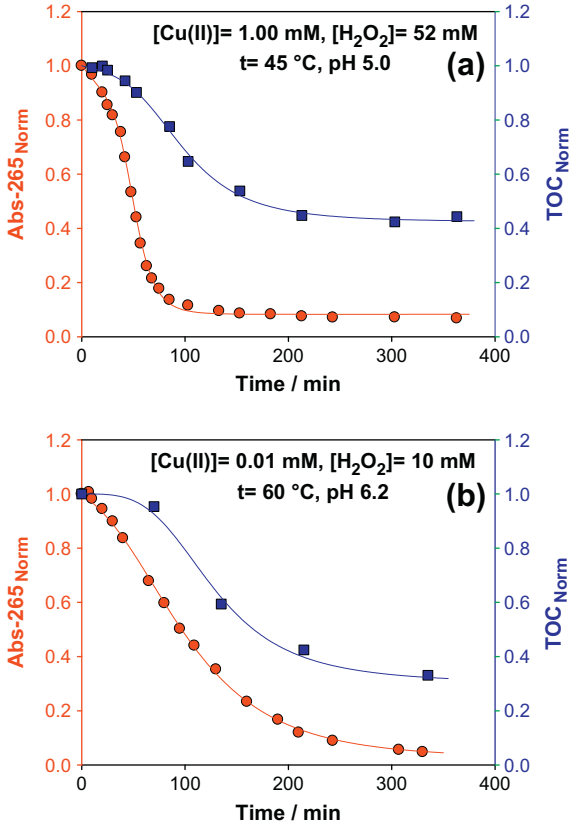

Fig. 5. Normalized profiles, of NBE (red circles) and TOC (blue squares), obtained in Cu(II)-based systems under different reaction conditions. (a) [H_2O_2] = 52 mM, [NBE] = 1.22 mM, [Cu(II)] = 1.00 mM, t = 45 °C and pH = 5.0. (b) [H_2O_2] = 10 mM, [NBE] = 1.22 mM, [Cu(II)] = 0.01 mM, t = 60 °C and pH = 6.2. (For interpretation of the references to color in this figure legend, the reader is referred to the web version of this article.)

ditions for copper(II)-catalyzed systems than for iron(III)-catalyzed systems. It is usually accepted that the formation of nitrophenols as primary products of NBE transformation occurs through a diffusion-controlled [45] addition of hydroxyl radicals to the aromatic NBE ring resulting in the formation of nitrohydroxycyclohexadienyl radicals (NHCHD·) [43,46,47]. This type of radical can undergo different reactions such as dimerization, disproportionation, oxygen addition to give the corresponding peroxy-radical or can participate in electron-transfer reactions with transition metals depending on the substituents in the aromatic ring and on the medium nature [23]. Hence, the analysis of the relative nitrophenol yields allows comparing the relative contribution of several parallel decay pathways of NHCHD· [43].

For copper-based systems, a pH change from 3.0 to 5.0 or the absence of dissolved oxygen shows negligible effects on product distribution. Moreover, the yields of copper-based systems operated under irradiation show relatively small differences in compar-

Table 2
Relative nitrophenol yields[a] and peak[b] DNB concentrations observed by HPLC analysis[c,d], for NBE treatment under different reaction conditions.

Entry	pH	Temp (°C)	[Cu(II)] (mM)	[Fe(III)] (mM)	[H_2O_2] (mM)	[NBE] (mM)	hν	O_2	$t^{½}_{NBE}$ (min)	η^N_{4NP}	η^N_{3NP}	η^N_{2NP}	$[DNB]_P$ (μM)
1	3.0	30	–	1.00	50	1.22	–	+	10	0.26	0.28	0.47	196
2	3.0	30	1.00	–	50	1.22	–	+	870	0.26	0.22	0.53	n.d.
3	5.0	30	1.00	–	50	1.22	–	+	247	0.27	0.24	0.49	n.d.
4	3.0	21	–	0.31	2.7	0.75	–	+	47	0.51	0.26	0.23	19.4
5	3.0	21	–	0.31	2.7	0.75	–	–	63	0.63	0.08	0.29	26.4
6	5.0	35	5.1	–	53	0.75	–	+	110	0.42	0.26	0.32	n.d.
7	5.0	35	5.1	–	53	1.22	–	–	129	0.43	0.26	0.31	n.d.
8	3.1	60	–	0.013	10	1.22	–	+	18	0.31	0.26	0.44	28.9
9	3.1	60	–	0.013	10	1.22	+	+	14	0.36	0.17	0.47	46.7
10	6.2	60	0.01	–	10	1.22	–	+	95	0.34	0.28	0.39	n.d.
11	6.2	60	0.01	–	10	1.22	+	+	37	0.45	0.31	0.25	n.d.

[a,b] Relative nitrophenol yields were calculated as $\eta^N_{XNP} = [nNP]_P/\Sigma_n[nNP]_P$, where $[nNP]_P$ are the peak concentrations of the nitrophenol isomers observed during the analyzed kinetic run. For all the experiments performed, the three nitrophenols peaked at the same time and for NBE conversion degrees of about 50%, whereas DNB concentration peaked at conversion degrees above 85%.

[c] Relative error in concentration measurements: 14%.

[d] Under the conditions tested, no significant amounts of phenol were detected.

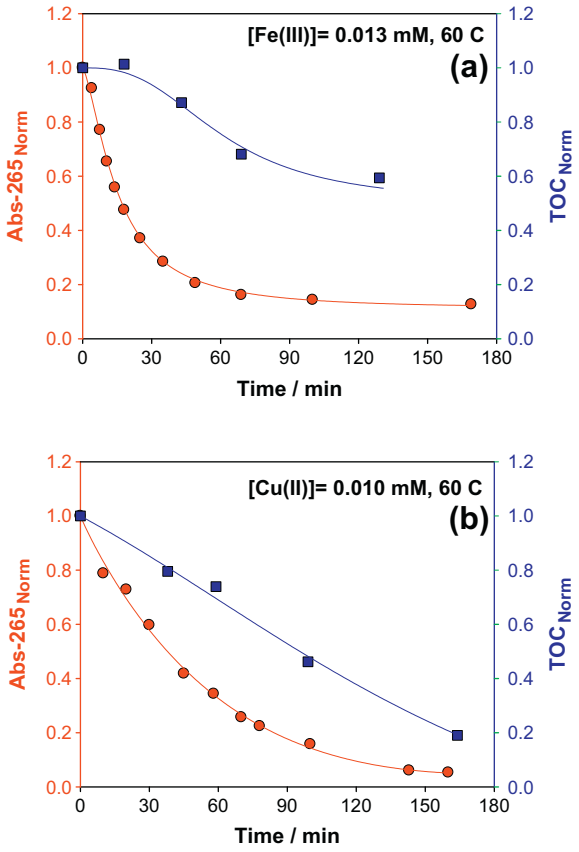

Fig. 6. Normalized profiles, of NBE (red circles) and TOC (blue squares), obtained at 60 °C under continuous irradiation ($\lambda > 310$ nm), in Fenton-like systems. (a) Fe(III) as photocatalyst: $[H_2O_2] = 10.4$ mM, [NBE] = 1.22 mM, [Fe(III)] = 0.014 mM and pH = 3.0. (b) Cu(II) as photocatalyst: $[H_2O_2] = 10.4$ mM, [NBE] = 1.22 mM, [Cu(II)] = 0.01 mM and pH = 6.2.

ison with the corresponding dark process. On the contrary, in Fe(III)-based treatments, the relative yield of 3-nitrophenol decreases noticeably in the absence of dissolved oxygen. The rather low yield of 3-nitrophenol observed for Fe(III)-catalyzed systems in the absence of dissolved oxygen has been attributed to the contribution of crossed disproportionation reactions where meta-NHCHD· radicals act as oxidizers with respect to para-NHCHD· or ortho-NHCHD· radicals, thus yielding 4-nitrophenol or 2-nitrophenol and nitrobenzene [43,46]. In this context, the negligible differences in product distributions observed for Cu(II)-catalyzed systems, operated either in the presence or in the absence of dissolved oxygen, suggest that the contribution of second order radical–radical reactions is of minor importance even under oxygen-free atmosphere.

3.5. Mineralization degree and spectral behavior

In order to compare the mineralization efficiency of Cu(II) or Fe(III)-based Fenton-like treatments in the absence of irradiation, total organic carbon measurements were performed for the experiments presented in Fig. 1 (i.e. 30 °C, pH 3.0 and identical initial concentrations). Once the final phase was reached, a TOC reduction of 24.4% was observed for the Fe(III)-catalyzed system. This is in line with previous reports showing that, in the absence of irradiation, TOC levels are only reduced by less than 25% and then remain practically constant [48–50]. On the other hand, the Cu(II)-catalyzed system achieved a much higher mineralization degree since a TOC reduction of 57.1% was recorded. A similar trend was reported for Cu(II)-catalyzed systems operated at 35 °C and pH 5.0, where TOC reductions of about 60% were observed [51].

The differences in the mineralization degrees can be explained by taking into account the properties of the complexes that each catalyst may form with some reaction intermediates. It is well known that, in Fenton and Fenton-like processes, carboxylic acids of low molecular weight may be formed by ring opening reactions during the degradation of aromatic compounds. In particular, oxalate forms very stable ferric complexes [52,53] that substantially hinder total mineralization in nonirradiated systems. Fe(III) in aqueous solution tends to form octahedral complexes and in excess of oxalate (a bidentate ligand), it generates the species $[Fe(C_2O_4)_3]^{3-}$, in which the six positions of the coordination sphere of the metal are occupied. The symmetry of the complex and the high affinity of Fe(III) by this ligand [54] result in the sequestration of the metal cation, making it inaccessible to H_2O_2 and hence blocking the reduction of Fe(III) to Fe(II). Conversely, due to its electron configuration, hexacoordinated Cu(II) tends to form severely distorted octahedral complexes with four short bonds located in one plane and two weakly bonded ligands located on the fifth and sixth positions [54,55]. These weakly bonded ligands might be more easily exchanged with H_2O_2 and the overall process would not be blocked.

The analysis of UV–vis absorption spectra obtained for the NBE degradation experiments performed in the presence of either Cu(II) or Fe(III) shows similar spectral evolutions during the initial degradation stages for both systems (Fig. S2, Supplementary material). However, the residual absorbance values at wavelengths above 280 nm during the final phase are much higher for the iron-catalyzed system than for the copper-catalyzed system. This result may be related to the differences in the complexation properties of each catalyst and also to the low mineralization degrees observed for the iron-based system. Therefore, the much higher residual absorbance values above 280 nm at the end of treatment in Fe(III)-based systems may be explained by taking into account the formation of Fe(III)-carboxylate complexes that typically exhibit ligand to metal charge-transfer absorption bands with high absorption coefficients up to 450 or 500 nm [56–58]. On the other hand, Cu(II)-carboxylate complexes exhibit lower absorption coefficients [59,60] and their formation would be less favored due to the higher degrees of mineralization achieved.

3.6. Potential application of copper-catalyzed systems

Given the relatively high toxicity of copper, it is clear that Fenton-like systems based on Cu(II) as catalyst should either use rather low copper concentrations or supported forms of the catalyst (i.e., heterogeneous copper-based Fenton-like systems). Taking into account the results presented in previous sections (i.e., the increase of catalytic activity at pH values above 4.5, the important effect of the working temperature and the relatively small influence of catalyst concentration), a new set of NBE degradation experiments, designed to test the potential application of copper ions in homogeneous phase was performed. Catalyst concentrations ranging from 1.0 to 0.01 mM, reaction temperatures between 45 and 60 °C and pH values from 3.0 to 7.0 were analyzed. Control experiments conducted in the absence of catalyst showed negligible changes in the shape of the solution spectra indicating that thermal activation of H_2O_2 may be neglected for the investigated timescales. In order to avoid evaporation losses and other complications in our experimental setup, 60 °C was chosen as the upper temperature limit. In addition, since the limits established by CAA, EPA and WHO for copper concentration in drinking water are between 1.0 and 2.0 mg/L [61–64], Cu(II) concentrations below 0.63 mg/L (i.e., 0.01 mM) were not tested.

3.6.1. Operation at near neutral pH values

Several researchers have already reported that there is a relatively narrow pH range (i.e., roughly 2.5–4.0) for iron(III)-based Fenton-like processes, the optimum working pH being about 2.8 [1,4,65]. At pH values lower than 2, reaction 4a slows down [7,66]; whereas for pH values above 4, Fe(III) precipitates as ferric hydroxides [7,66] and the process becomes less effective. On the contrary, it has been reported that copper-catalyzed systems can effectively activate H_2O_2 above pH 4.5 and even in alkaline conditions [18,29,38,39].

In order to assess the optimum pH for NBE degradation using Cu(II) as catalyst, we performed a set of experiments with initial pH values ranging from 3.0 to 7.0, but using constant concentrations of NBE, H_2O_2 and Cu(II). Within the experimental domain analyzed, solutions showed no turbidity or evidence of precipitate formation, thus indicating that Cu(II) remained in solution. Fig. 4a shows the concentration profiles obtained using different initial pH values, whereas Fig. 4b plots the effect of the initial pH on the overall NBE degradation rate (r^{NBE}).

In contrast to Fe(III), Cu(II) is catalytically active in a wider range of initial pH values. Moreover, the highest activity is evidenced at near neutral pH values (around 6.2). Noteworthy, although the results shown in Fig. 4 were obtained using a working temperature of 60 °C, a similar trend was previously reported for NBE degradation in Cu(II)-based systems operated at much lower temperature (i.e., 20 °C) [51].

A possible explanation of the effect of the solution pH on the catalytic activity in Cu(II)-based systems may be given by considering the pKa value of the acid–base equilibrium $HO_2^{\cdot}/O_2^{\cdot-}$ (i.e., 4.85 [4]), the differences in the rate constant values associated with reactions 5b and 6b, and the speciation of copper(II) [9,18]. Hence, as the pH increases from 4 to 6, the fraction of $O_2^{\cdot-}$ substantially increases and Cu(II) reduction becomes faster since $k_{R6b} > k_{R5b}$, whereas beyond pH 7 the fraction of soluble Cu(II) significantly decreases and turns negligible at pH > 8 [67].

The capability of working at near neutral pH values is a rather important result concerning technical applications of copper(II)-based systems, since many industrial effluents exhibit pH values near neutrality and homogenous Fenton-like treatments based on iron(III) as catalyst would require a previous acidification stage and subsequent re-neutralization, thus increasing the associated operating costs.

The wide pH range of catalytic activity exhibited by Cu(II) may result advantageous for effluents with relatively high organic contents, since the pH may vary along the treatment due to the formation of reaction intermediates. Interestingly, this is the case for the studied system since, for experiments initiated with the optimal value, pH typically decreased towards values below 4 along NBE treatment (Table S2, Supplementary material). To test whether this pH evolution negatively affected the efficiency of the process, we performed an additional experiment under identical initial conditions but in the presence of a buffer. The kinetic profiles (Fig. S3, Supplementary material) show that the pH decrease recorded for the non-buffered system does not appreciably affect the overall treatment time. This is an important result regarding technical applications since no pH control would be required to sustain the catalytic activity of Cu(II) throughout NBE treatment.

3.6.2. Working temperature and catalyst concentration

With the aim of assessing working conditions that allow reasonable NBE treatment times using low catalyst concentrations, the effects of catalyst and oxidant concentrations were analyzed at 45 and 60 °C (Fig. S4, Supplementary material). As expected, treatment times decreased with increasing working temperature, catalyst concentration and oxidant concentration. It is worth mentioning that, in line with the results obtained below 40 °C (Section 3.3), the treatment times showed low sensibility to a decrease in the catalyst concentration.

The analysis of the entire set of results obtained in the present work suggests that, within the experimental domain analyzed, the best operative conditions for practical applications of copper-based systems should involve the use of high reaction temperatures, near neutral initial pH values and low catalyst concentrations. In order to confirm this hypothesis, we compared the kinetic profiles obtained at pH 5.0 and 45 °C in the presence of rather high concentrations of both Cu(II) and H_2O_2 with those obtained at pH 6.2 and 60 °C in the presence of much lower catalyst and oxidant concentrations (Fig. 5).

Although the 60 °C experiment was performed using substantially lower concentrations of catalyst and oxidant than those used in the 45 °C experiment (i.e., 5.2 times less oxidant and 100 times less catalyst), similar timescales were required to reach absorbance decreases of 90%. Moreover, the mineralization degree was around 70% for the low concentration-high temperature experiment, whereas TOC reduction was only 60% for the high concentration-low temperature experiment. In other words, a moderate increase in the operation temperature (only 15 °C) allowed obtaining higher mineralization efficiencies even though the catalyst concentration was reduced by two orders of magnitude and the operative costs associated with the oxidant employed were reduced by 80%.

3.7. Photo-enhanced Fenton-like systems

It is well known that the efficiency of iron(III)-based Fenton-like systems can be substantially enhanced in the presence of UV or visible irradiation [14,48,49]. The enhancement is because the strong ferric complexes formed with the degradation intermediates are photochemically active with high absorption coefficients and high quantum yields of Fe(II) production [1,49,68,69]. In addition, depending on the irradiation wavelength, photochemical processes such as H_2O_2 photolysis and substrate photolysis may also play some role in photo-enhanced systems.

In order to make a fair comparison between the efficiencies of both catalysts in photo-Fenton systems, NBE degradation experiments were carried out at 60 °C using identical concentrations of NBE and H_2O_2, very similar catalyst concentrations and initial pH around the optimal values for each catalyst. The mole ratio H_2O_2/NBE used in these experiments was lower than 10, although the theoretical mole ratio H_2O_2/NBE required to completely mineralize NBE, in the absence of other oxidants, is 15. For economical reasons, some Fenton systems have been operated with substoichiometric amounts of H_2O_2 and under continuous air supply in order to partially replace H_2O_2 by O_2 [1,70]. In addition, substrate degradation in the absence of oxygen supply is somewhat slower than that observed under continuous supply of O_2 [65,70–75]. Dissolved oxygen is consumed in several oxidative reaction steps that are triggered either by the attack of $HO^{\cdot}$ to the target substrate and its intermediate degradation products [4,43,44,71,76] or by organic radicals generated by photoredox steps such as photoinduced ligand-to-metal electron-transfer reactions [21]. Therefore, our irradiation experiments were conducted under continuous air supply. It should be pointed out that control experiments, carried out in the dark at 60 °C and using the same reagent concentrations but in the absence of catalyst, showed small evaporation losses due to the continuous air supply, the total loss of NBE being less than 9.6% after 2 h.

The comparison of the kinetic profiles (Fig. 6) shows that very similar timescales are required to achieve a reduction of 90% of the initial absorbance. However, substantial differences in the mineralization degrees are observed since, for NBE conversion degrees close to 100%, TOC reduction in the presence of Fe(III) is only 40%, whereas TOC reduction in the presence of Cu(II) is about 80%.

It is worth mentioning that rather small residual absorbance values (less than 0.2) were obtained in both systems. For Fe(III)-catalyzed systems, this is in contrast to what is seen in Figs. 1 and 3. The differences in spectral behavior observed for Fe(III)-based systems may be explained by taking into account the photolysis of Fe(III)-carboxylate complexes. Additionally, given the rather low catalyst concentrations used in the photochemical experiments performed at 60 °C, Fe(III)-carboxylate species, if formed, would have a very small contribution to the total absorbance.

A final comment regarding DNB formation should be added. The amount of 1,3-dinitrobenzene formed in iron(III)-catalyzed systems was higher under irradiation than in the dark (entries 8 and 9, Table 2). This may be of major concern from an environmental perspective. Nevertheless, no DNB was detected in copper(II)-catalyzed systems either in the presence or in the absence of irradiation. Hence, the Cu(II)-catalyzed systems seem more attractive when production of less toxic organic intermediates is desired.

4. Conclusions

Nitrobenzene can be completely oxidized in Fenton-like systems based on the use of Cu(II) or Fe(III) as catalysts. In order to obtain comparable transformation rates at temperatures below 30 °C, more severe conditions are required in the presence of Cu(II) than in the presence of Fe(III). However, Cu(II) is catalytically active in a wide range of pH values around neutrality and above 35 °C it exhibits a rather high apparent activation energy. For both catalysts, a higher substrate concentration leads to an increase in the treatment time, whereas increasing oxidant or catalyst concentrations leads to higher overall reaction rates. While the effects of catalyst and substrate concentrations are more pronounced for Fe(III)-based systems, the effect of oxidant concentration is more evident for Cu(II)-based systems.

The aforementioned differences bring about important consequences for potential applications, since Cu(II)-based Fenton-like systems are expected to show high degradation efficiencies when operated at near neutral pH, moderate reaction temperatures and low catalyst concentrations.

The reductions of total organic carbon content were higher in Cu(II)-based systems than in Fe(III)-based systems. This behavior may be explained by considering differences in the properties of the complexes that each catalyst may form with intermediate degradation products. In addition, 1,3-dinitrobenzene was not detected in copper(II)-catalyzed systems. Therefore, Cu(II) seems more attractive for achieving high TOC reductions and low production of toxic organic intermediates during the oxidative transformation of nitroaromatic compounds.

The kinetic and mechanistic differences observed between Fe(III)-based and Cu(II)-based Fenton-like systems suggest that the use of Cu(II) may result advantageous for certain specific applications, especially taking into account that 60 °C is a temperature easily achievable in industrial processes. In addition, circumventing pH adjustments as well as avoiding the use of irradiation undoubtedly simplify reactor designs and also decrease both implementation and operating costs. Finally, the results reported here leave the door open for further investigations concerning the use of Cu(II) as a versatile catalyst in both Fenton-like and photo-Fenton systems operated at low concentrations, neutral pH and moderate temperatures.

Acknowledgements

The authors would like to thank the Reviewers for their helpful comments and Dr. Luciano Carlos for his valuable suggestions. This research was partially supported by the ANPCyT (Project No. PICT 1435, Argentina), the CONICET (Project No. PIP 0425, Argentina) and the UNLP (Project No. X559, Argentina). M.R.C. thanks CONICET for a graduate studentship. D.A.N. and A.M.B. thank CONICET for their postdoctoral fellowships. M.P.J. and F.S.G.E. are research members of CONICET, Argentina.

Appendix A. Supplementary material

Supplementary data associated with this article can be found, in the online version, at http://dx.doi.org/10.1016/j.cej.2013.05.002.

References

[1] S. Malato, P. Fernández-Ibáñez, M.I. Maldonado, J. Blanco, W. Gernjak, Decontamination and disinfection of water by solar photocatalysis: Recent overview and trends, Catal. Today 147 (2009) 1–59.
[2] M. Pera-Titus, V. García-Molina, M.A. Baños, J. Giménez, S. Esplugas, Degradation of chlorophenols by means of advanced oxidation processes: a general review, Appl. Catal. B 47 (2004) 219–256.
[3] O. Legrini, E. Oliveros, A.M. Braun, Photochemical processes for water treatment, Chem. Rev. 93 (1993) 671–698.
[4] J.J. Pignatello, E. Oliveros, A. MacKay, Advanced oxidation processes for organic contaminant destruction based on the Fenton reaction and related chemistry, Crit. Rev. Anal. Chem. 36 (2006) 1–84.
[5] C. Walling, Fenton's reagent revisited, Acc. Chem. Res. 8 (1975) 125–131.
[6] C.K. Duesterberg, W.J. Cooper, T.D. Waite, Fenton-mediated oxidation in the presence and absence of oxygen, Environ. Sci. Technol. 39 (2005) 5052–5058.
[7] J. De Laat, H. Gallard, Catalytic decomposition of hydrogen peroxide by Fe(III) in homogeneous aqueous solution: mechanism and kinetic modeling, Environ. Sci. Technol. 33 (1999) 2726–2732.
[8] J. De Laat, T. Giang Le, Effects of chloride ions on the iron(III)-catalyzed decomposition of hydrogen peroxide and on the efficiency of the Fenton-like oxidation process, Appl. Catal. B 66 (2006) 137–146.
[9] J.W. Moffett, R.G. Zika, Reaction kinetics of hydrogen peroxide with copper and iron in seawater, Environ. Sci. Technol. 21 (1987) 804–810.
[10] M. Masarwa, H. Cohen, D. Meyerstein, D.L. Hickman, A. Bakac, J.H. Espenson, Reactions of low-valent transition-metal complexes with hydrogen peroxide. Are they "Fenton-like" or not? 1. The case of Cu+aq and Cr2+aq, JACS 110 (1988) 4293–4297.
[11] X. Hu, F.L.Y. Lam, L.M. Cheung, K.F. Chan, X.S. Zhao, G.Q. Lu, Copper/MCM-41 as catalyst for photochemically enhanced oxidation of phenol by hydrogen peroxide, Catal. Today 68 (2001) 129–133.
[12] J. Soler, A. Garcıí-Ripoll, N. Hayek, P. Miró, R. Vicente, A. Arques, A.M. Amat, Effect of inorganic ions on the solar detoxification of water polluted with pesticides, Water Res. 43 (2009) 4441–4450.
[13] F.S. García Einschlag, J. Lopez, L. Carlos, A.L. Capparelli, A.M. Braun, E. Oliveros, Evaluation of the efficiency of photodegradation of nitroaromatics applying the UV/H_2O_2 technique, Environ. Sci. Technol. 36 (2002) 3936–3944.
[14] L. Carlos, D. Fabbri, A.L. Capparelli, A. Bianco Prevot, E. Pramauro, F. García Einschlag, Effect of simulated solar light on the autocatalytic degradation of nitrobenzene using Fe^{3+} and hydrogen peroxide, J. Photochem. Photobiol., A 201 (2009) 32–38.
[15] D. Nichela, L. Carlos, F. García Einschlag, Autocatalytic oxidation of nitrobenzene using hydrogen peroxide and Fe(III), Appl. Catal. B 82 (2008) 11–18.
[16] W.G. Barb, J.H. Baxendale, P. George, K.R. Hargrave, Reactions of ferrous and ferric ions with hydrogen peroxide. Part II.—The ferric ion reaction, Trans. Faraday Soc. 47 (1951) 591–616.
[17] R.D. Gray, Kinetics of oxidation of copper(I) by molecular oxygen in perchloric acid-acetonitrile solutions, JACS 91 (1969) 56–62.
[18] F.J. Millero, V.K. Sharma, B. Karn, The rate of reduction of copper(II) with hydrogen peroxide in seawater, Mar. Chem. 36 (1991) 71–83.
[19] J.F. Perez-Benito, Reaction pathways in the decomposition of hydrogen peroxide catalyzed by copper(II), J. Inorg. Biochem. 98 (2004) 430–438.
[20] M. González-Dávila, J.M. Santana-Casiano, A.G. González, N. Pérez, F.J. Millero, Oxidation of copper(I) in seawater at nanomolar levels, MAR. CHEM. 115 (2009) 118–124.
[21] P. Cieśla, P. Kocot, P. Mytych, Z. Stasicka, Homogeneous photocatalysis by transition metal complexes in the environment, J. Mol. Catal. A: Chem. 224 (2004) 17–33.
[22] K. Stemmler, U. von Gunten, OH radical-initiated oxidation of organic compounds in atmospheric water phases: Part 2. Reactions of peroxyl radicals with transition metals, Atmos. Environ. 34 (2000) 4253–4264.
[23] R. Chen, J.J. Pignatello, Role of quinone intermediates as electron shuttles in Fenton and photoassisted Fenton oxidations of aromatic compounds, Environ. Sci. Technol. 31 (1997) 2399–2406.
[24] D. Nichela, M. Haddou, F. Benoit-Marquié, M.-T. Maurette, E. Oliveros, F.S. García Einschlag, Degradation kinetics of hydroxy and hydroxynitro derivatives of benzoic acid by Fenton-like and photo-Fenton techniques: a comparative study, Appl. Catal. B 98 (2010) 171–179.
[25] O. Primo, M.J. Rivero, I. Ortiz, Photo-Fenton process as an efficient alternative to the treatment of landfill leachates, J. Hazard. Mater. 153 (2008) 834–842.

[26] M. Neamtu, A. Yediler, I. Siminiceanu, A. Kettrup, Oxidation of commercial reactive azo dye aqueous solutions by the photo-Fenton and Fenton-like processes, J. Photochem. Photobiol., A 161 (2003) 87–93.
[27] J. Gabriel, P. Baldrian, P. Verma, T. Cajthaml, V. Merhautová, I. Eichlerová, I. Stoytchev, T. Trnka, P. Stopka, F. Nerud, Degradation of BTEX and PAHs by Co(II) and Cu(II)-based radical-generating Systems, Appl. Catal. B 51 (2004) 159–164.
[28] V. Shah, P. Verma, P.S.J. Gabriel, P. Baldrian, F. Nerud, Decolorization of dyes with copper(II)/organic acid/hydrogen peroxide systems, Appl. Catal. B 46 (2003) 287–292.
[29] L. Santos-Juanes, A.M. Amata, A. Arques, A. Bernabeu, M. Silvestre, R. Vicente, E. Añó, Activated sludge respirometry to assess solar detoxification of a metal finishing effluent, J. Hazard. Mater. 153 (2008) 905–910.
[30] EPA, Code of Federal Regulations. Title 40 – Protection of Environment, in: E.P.A. (EPA) (Ed.), 2004.
[31] O.A. O'Connor, L.Y. Young, Toxicity and anaerobic biodegradability of substituted phenols under methanogenic conditions, Environ. Toxicol. Chem. 8 (1989) 853–862.
[32] WHO, Environmental Health Criteria 230 – Nitrobenzene Part. 1, in: World Health Organization, 2003.
[33] EPA, Ambient Water Criteria for Nitrophenols, in: United States Environmental Protection Agency, Washington, DC, 1980.
[34] R. Snyder, Ethel Browning's Toxicity and Metabolism of Industrial Solvents, second ed., Elsevier Science, 1987.
[35] C.C. Allain, L.S. Poon, C.S.G. Chan, W. Richmond, P.C. Fu, Enzymatic determination of total serum cholesterol, Clin. Chem. 20 (1974) 470–475.
[36] F.S. García Einschlag, L. Carlos, A.L. Capparelli, A.M. Braun, E. Oliveros, Degradation of nitroaromatic compounds by the UV–H_2O_2 process using polychromatic radiation sources, Photochem. Photobiol. Sci. 1 (2002) 520–525.
[37] H.J. Kuhn, S.E. Braslavsky, R. Schmidt, Chemical actinometry, Pure Appl. Chem. 76 (2004) 2105–2146.
[38] M.H. Robbins, R.S. Drago, Activation of hydrogen peroxide for oxidation by copper(II) complexes, J. Catal. 170 (1997) 295–303.
[39] F. Nerud, P. Baldrian, J. Gabriel, D. Ogbeifun, Decolorization of synthetic dyes by the Fenton reagent and the Cu/pyridine/H_2O_2 system, Chemosphere 44 (2001) 957–961.
[40] S.K. Scott, Oscillations, Waves and Chaos in Chemical Kinetics, Oxford Science Publications, Oxford, 1994.
[41] Y. Du, M. Zhou, L. Lei, Role of the intermediates in the degradation of phenolic compounds by Fenton-like process, J. Hazard. Mater. 136 (2006) 859–865.
[42] F. Chen, W. Ma, J. He, J. Zhao, Fenton degradation of malachite green catalyzed by aromatic additives, J. Phys. Chem. A 106 (2002) 9485–9490.
[43] L. Carlos, D. Fabbri, A.L. Capparelli, A. Bianco Prevot, E. Pramauro, F.S. García Einschlag, Intermediate distributions and primary yields of phenolic products in nitrobenzene degradation by Fenton's reagent, Chemosphere 72 (2008) 952–958.
[44] L. Carlos, D. Nichela, J.M. Triszcz, J.I. Felice, F.S. García Einschlag, Nitration of nitrobenzene in Fenton's processes, Chemosphere 80 (2010) 340–345.
[45] J. Hoigne, Inter-calibration of OH radical sources and water quality parameters, Water Sci. Technol. 35 (1997) 1–8.
[46] K. Bhatia, Hydroxyl radical induced oxidation of nitrobenzene, J. Phys. Chem. 79 (1975) 1032–1038.
[47] M.L. Rodriguez, V.I. Timokhin, S. Contreras, E. Chamarro, S. Esplugas, Rate equation for the degradation of nitrobenzene by 'Fenton-like' reagent, Adv. Environ., Res. 7 (2003) 583–595.
[48] A. Serra, X. Domènech, C. Arias, E. Brillas, J. Peral, Oxidation of a-methylphenylglycine under Fenton and electro-Fenton conditions in the dark and in the presence of solar light, Appl. Catal. B 89 (2009) 12–21.
[49] V. Kavitha, K. Palanivelu, Degradation of nitrophenols by Fenton and photo-Fenton processes, J. Photochem. Photobiol. A 170 (2005) 83–95.
[50] M.S. Lucas, J.A. Peres, Decolorization of the azo dye Reactive Black 5 by Fenton and photo-Fenton oxidation, Dyes Pigm. 71 (2006) 236–244.
[51] D.A. Nichela, Estudio del mecanismo y la cinética de degradación de contaminantes aromáticos empleando reacciones tipo Fenton, Electro-Fenton y Foto-Fenton, in: Facultad de Ciencias Exactas, Departamento de Química, Universidad Nacional de La Plata, La Plata, 2010, pp. 224.
[52] E. Brillas, I. Sirés, M.A. Oturan, Electro-Fenton process and related electrochemical technologies based on Fenton's Reaction Chemistry, Chem. Rev. 109 (2009) 6570–6631.
[53] G. Zhang, F. Yang, L. Liu, Comparative study of Fe^{2+}/H_2O_2 and Fe^{3+}/H_2O_2 electro-oxidation systems in the degradation of amaranth using anthraquinone/polypyrrole composite film modified graphite cathode, J. Electroanal. Chem. 632 (2009) 154–161.
[54] F.A. Cotton, G. Wilkinson, Química Inorgánica Avanzada, Editorial Limusa, S.A. de C.V. Grupo Noriega Editores, Balderas, 1996.
[55] B. Jasiewicz, B. Warżajtis, U. Rychlewska, From four to five and six coordinated sparteine and α-isosparteine mononuclear Cu(II) complexes through the carboxylate donors, Polyhedron 30 (2011) 1703–1709.
[56] S.J. Hug, H.-U. Laubscher, B.R. James, Iron(III) catalyzed photochemical reduction of chromium(VI) by oxalate and citrate in aqueous solutions, Environ. Sci. Technol. 31 (1997) 160–170.
[57] I.P. Pozdnyakov, O.V. Kel, V.F. Plyusnin, V.P. Grivin, N.M. Bazhin, New insight into photochemistry of ferrioxalate, J. Phys. Chem. A 112 (2008) 8316–8322.
[58] K. Kuma, S. Nakabayashi, K. Matsunaga, Photoreduction of Fe(III) by hydroxycarboxylic acids in seawater, Water Res. 29 (1995) 1559–1569.
[59] X. Peng, G.-H. Cui, D.-J. Li, S.-Z. Wu, Y.-M. Yu, Structure, spectroscopy, and theory calculations of mononuclear mixed-ligand copper(II) complex with malonate and 2-propylimidazole, [Cu(mal)(PIM)2(H_2O)], J. Mol. Struct. 971 (2010) 47–52.
[60] L. Sun, C.-H. Wu, B.C. Faust, Photochemical redox reactions of inner-sphere copper(II)-dicarboxylate complexes: effects of the dicarboxylate ligand structure on copper(I) quantum yields, J. Phys. Chem. A 102 (1998) 8664–8672.
[61] CAA Código Alimentario Argentino, in, <http://www.anmat.gov.ar/alimentos/codigoa/CAPITULO_XII.pdf>.
[62] REPÚBLICA DE ARGENTINA. DECRETO NACIONAL: 831/93. Reglamentación de Residuos Peligrosos, in, 1993.
[63] EPA, Basic Information about Copper in Drinking Water, in, United States Environmental Protection Agency.
[64] WHO, Copper in Drinking-water Background document for development of WHO Guidelines for Drinking-water Quality, in: World Health Organization, 2004.
[65] J.J. Pignatello, Dark and photoassisted iron(3+)-catalyzed degradation of chlorophenoxy herbicides by hydrogen peroxide, Environ. Sci. Technol. 26 (1992) 944–951.
[66] C. Jiang, S. Pang, F. Ouyang, J. Ma, J. Jiang, A new insight into Fenton and Fenton-like processes for water treatment, J. Hazard. Mater. 174 (2010) 813–817.
[67] K. Powell, P.L. Brown, R.H. Byrne, T. Gajda, G. Hefter, S. Sjöberg, H. Wanner, Chemical speciation of environmentally significant metals with inorganic ligands. Part 2: The Cu^{2+}–OH^-, Cl^-, CO_3^{2-}, SO_4^{2-}, and PO_4^{3-} systems, Pure Appl. Chem. 79 (2007) 895–950.
[68] D. Prato-Garcia, R. Vasquez-Medrano, M. Hernandez-Esparza, Solar photoassisted advanced oxidation of synthetic phenolic wastewaters using ferrioxalate complexes, Solar Energy 83 (2009) 306–315.
[69] M. Skoumal, C. Arias, P.L. Cabot, F. Centellas, J.A. Garrido, R.M. Rodríguez, E. Brillas, Mineralization of the biocide chloroxylenol by electrochemical advanced oxidation processes, Chemosphere 71 (2008) 1718–1729.
[70] B. Utset, J. Garcia, J. Casado, X. Doménech, J. Peral, Replacement of H_2O_2 by O_2 in Fenton and photo-Fenton reactions, Chemosphere 41 (2000) 1187–1192.
[71] Y. Sun, J.J. Pignatello, Photochemical Reactions Involved in the Total Mineralization of 2,4-D by Fe^{3+}/H_2O_2/UV, Environ. Sci. Technol. 27 (1993) 304–310.
[72] M. Haddou, F. Benoit-Marquié, M.-T. Maurette, E. Oliveros, Oxidative degradation of 2,4-dihydroxybenzoic acid by the Fenton and Photo-Fenton processes: kinetics, mechanisms, and evidence for the substitution of H_2O_2 by O_2, Helv. Chim. Acta 93 (2010) 1067–1080.
[73] D.L. Sedlak, A.W. Andren, Oxidation of Chlorobenzene with Fenton's Reagent, Environ. Sci. Technol. 25 (1991) 777–782.
[74] F.J. Rivas, F.J. Beltrán, O. Gimeno, P. Alvarez, Treatment of brines by combined Fenton's reagent–aerobic biodegradation II. Process modeling, J. Hazard. Mater. 96 (2003) 259–276.
[75] Y. Du, M. Zhou, L. Lei, The role of oxygen in the degradation of p-chlorophenol by Fenton system, J. Hazard. Mater. 139 (2007) 108–115.
[76] A.A. Burbano, D.D. Dionysiou, M.T. Suidan, Effect of oxidant-to-substrate ratios on the degradation of MTBE with Fenton reagent, Water Res. 42 (2008) 3225–3239.